

**A GENERALIZED CONSTITUTIVE MODEL FOR A V-4Cr-4Ti ALLOY – E. Donahue,
G.R. Odette, G.E. Lucas (University of California, Santa Barbara)**

OBJECTIVE

The objective of this work is to develop a generalized constitutive equation for a V-4Cr-4Ti alloy that can be used in conjunction with Finite Element Methods to predict crack tip stress and strain fields as a function of temperature and loading rate.

SUMMARY

A physically based constitutive model for low-to-intermediate temperatures, strains and strain rates is derived for the program heat of the V-4Cr-4Ti. The supporting database is based on tensile tests carried out over a wide range of temperatures and strain rates. The overall constitutive model is based on additive yield and post yield strain hardening contributions to the flow stress. The yield stress has both thermally activated and athermal components. The former can be described by a two-mechanism activated dislocation slip model, with contributions from both lattice friction (lower temperature) and interstitial obstacles (higher temperature). The model uses a weighted average of the two mechanisms as a function of a strain rate compensated temperature. Post-yield strain hardening was found to be essentially athermal. Strain hardening can be fit by a two-component modified Voce-type model, which predicts saturating hardening behavior. The constitutive model is used to determine flow stability limits as estimates of uniform tensile strains. The relatively compact, but mechanism-based, model has a number of both fundamental and practical advantages that are briefly outlined. Extensions to directly model compositionally and microstructurally mediated mechanisms, including the effects of irradiation, and key phenomena, such as flow localization, are important objectives of future research.

PROGRESS AND STATUS

Introduction

Constitutive properties are required for design and to measure, apply and obtain a basic understanding of a long list of life-limiting failure-related properties and parameters, such as fracture toughness. In this work we develop a constitutive description of a V-4Cr-4Ti alloy in the *unirradiated* condition for low-to-intermediate temperatures and strain rates (i.e., outside the creep and strain aging regimes). Specifically, we seek a model that accurately and compactly describes the effects of temperature (T), strain rate ($\dot{\epsilon}$) and strain (ϵ) on the uniaxial flow stress, $\sigma_{11}(T, \dot{\epsilon}, \epsilon)$ underpinned by dislocation dynamics theories. The research involved three steps: a) measuring and properly reducing the requisite tensile data base; b) analyzing the general data trends in the context of simple, but physically-based, analytical formulations of constitutive models; and c) quantitatively fitting the model equations to the data base.

Experimental Procedures and Data Reduction

Details of the materials and test methods for a wide range of temperatures and strain rates are described elsewhere [1].

Results and Analysis

Representative stress–strain curves have been reported previously [2]. Development of the model equations follow the approach of Armstrong [3]. This model divides flow stress (σ_{fl}) into yield (σ_y) and post yield (σ_ϵ), strain hardening, contributions. The σ_y is composed of strongly and weakly temperature-strain rate sensitive components as

$$\sigma_y(T, \dot{\epsilon}) = \sigma_{yt}(T, \dot{\epsilon}) + \sigma_{ya} \quad (1)$$

The development of post-yield dislocation structures results in a strain hardening component, σ_ϵ . For bcc single crystal crystals with low dislocation densities, σ_ϵ also depends on $\dot{\epsilon}$ and T [4], suggesting a general form:

$$\sigma_{fl}(T, \dot{\epsilon}, \epsilon) = \sigma_{yt}(T, \dot{\epsilon}) + \sigma_{ya} + \sigma_\epsilon(T, \dot{\epsilon}, \epsilon) \quad (2)$$

The (low) temperature-(high) strain rate dependence of σ_y in bcc metals and alloys is attributed to the low mobility of screw dislocations which experience a high Peierls, or lattice friction, resistance to slip [5]. The corresponding trade-off between temperature T and $\dot{\epsilon}$ can be represented in terms of a strain rate compensated temperature (T') where

$$T' = T [1 + C \ln(\dot{\epsilon} / \dot{\epsilon}_r)] \quad (3)$$

Here T is the actual absolute temperature (K) for the reference strain rate, $\dot{\epsilon}_r$.

Taking the slowest strain rate of 4×10^{-4} /s as the reference condition, the σ_y data at all three strain rates were plotted on T' scale, using the 'best fit' value for C = 0.030 the T' as shown in Figure 1. For a single underlying thermally activated kink nucleation mechanism the simplest fit form is [6],

$$\sigma_y(T') = \sigma_i [1 - (T'/T_c)] + \sigma_a \quad (4)$$

where σ_i and σ_a are the thermal and athermal yield stress contributions at 0°K. However, dispersed barrier strengthening by interstitial solutes is also important, particularly at higher temperatures. T' -weighted averaging and fitting σ_i and T_c for two (1 and 2) activated processes was used to model $\sigma_y(T')$ as

$$\sigma_y(T') = [\sigma_{i1} - (\sigma_{i1} - \sigma_{i2})T'/T_{c2}] [1 - T' / \{T_{c1} + (T_{c2} - T_{c1})T'/T_{c2}\}] + \sigma_a (1 - \beta T) \quad (5)$$

The best fit results are shown as the solid curve in Figure 1 for: a) $\sigma_{y11} = 780$ and $\sigma_{y12} = 110$ MPa; $\sigma_a = 255$ MPa; b) $T_{c1} = 188$ and $T_{c2} = 500$ °K; and $\beta = 6 \times 10^{-5}$ or

$$\sigma_y(T') = 1035 - 1.32T' + (1.32T' - 780)T' / (188 + 0.624T') \quad (\text{MPa}) \quad (6)$$

The post yield strain hardening contribution was experimentally defined for plastic strain levels of 0.5 to 3.0% in increments of 0.5% and from 3.0 to 14.0% in increments of 1.0% as

$$\sigma_\epsilon(T', \epsilon) = \sigma_{fl}(T', \epsilon) - \sigma_y(T') \quad (7)$$

To a good approximation σ_ϵ can be treated as being athermal. The corresponding $\sigma_\epsilon(\epsilon)$ averaged over T' for the 17 ϵ levels is shown in Figure 3. Two regimes above and below an ϵ of about 0.025 are observed. This was fit with a modified two-term Voce type equation [7] with the general form

$$\sigma_{\varepsilon}(\varepsilon) = \chi_{\varepsilon 1} \varepsilon^{p_1} [1 - \exp(-\varepsilon_{s1}/\varepsilon)] + \chi_{\varepsilon 2} (\varepsilon - \varepsilon_1 \geq 0)^{p_2} [1 - \exp(-\varepsilon_{s2}/\varepsilon)] \quad (8)$$

Here $\chi_{\varepsilon 1}$ and $\chi_{\varepsilon 2}$ represent the magnitude of each strain hardening term, p_1 and p_2 are the corresponding power law, ε_{s1} and ε_{s2} are the flow stress saturation strains, and ε_1 is the threshold strain for the second mechanism. The solid line in Figure 3 is a best fit given by the expression for: $\chi_{\varepsilon 1} = 865$ MPa, $\chi_{\varepsilon 2} = 110$ MPa; $p_1 = p_2 = 1$; $\varepsilon_{s1} = 0.07$, $\varepsilon_{s2} = 0.23$; and $\varepsilon_1 = 0.025$.

Equations 3, 6 and 8 define an overall constitutive model,

$$\sigma_{fl}(T, \dot{\varepsilon}, \varepsilon) = 1035 - 1.32T' + \{(1.32T' - 780T')/(188 + 0.624T')\} + 865\varepsilon[1 - \exp(-0.07/\varepsilon)] + 110(\varepsilon - 0.025)[1 - \exp(-0.023/\varepsilon)] \text{ (MPa)} \quad (9)$$

Predicted versus measured σ_{fl} at ε of 0.5, 1, 2, 4, 8 and 14% are shown in Figure 3. The overall standard deviation of the predicted versus measured σ_{fl} is ± 9.1 MPa. The model can be applied over the combined T and $\dot{\varepsilon}$ range to 100°C, 2/sec respectively.

Figure 4 shows the ε_u data plotted against σ_y . Except in two cases ε_u ranges from about 0.10 to 0.18. The exceptions were for the highest strain rate case at low temperatures of -132 and -196°C. In this case adiabatic heating may contribute to flow localization and the low ε_u . The constitutive model can be used compute ε_u based on the criteria that $dP/d\varepsilon \leq 0$. The dashed line in Figure 4 is the nominal predicted ε_u . While the trends are reasonable, the simple model over-predicts the measured values. This discrepancy suggests that ε_u is influenced by either defects and other inhomogenities in the specimens, or an inherent propensity towards flow localization. These effects can be treated by a phenomenologically by increasing the effective rate of reduction in load bearing area per unit strain by a constant factor. The solid line in Figure 4 shows the corresponding results for a factor of 1.6

Discussion, Summary and Conclusions

The σ_{fl} for the program heat of V-4Cr-4Ti alloy has a classical low-temperature activated σ_{yt} regime and athermal contributions to both σ_y and σ_{ε} . The athermal post-yield σ_{ε} follows a two component Voce-type hardening law. Overall, the model, which incorporates analytical expressions for these processes that are fit to the tensile database, is broadly consistent with current understanding of deformation in bcc alloys. The relatively simple and compact form of the constitutive model has a number of practical and fundamental advantages as discussed elsewhere [1]. Developing microstructurally based constitutive models, including the effects of irradiation, and key phenomena such as flow localization, is an important objective of future research.

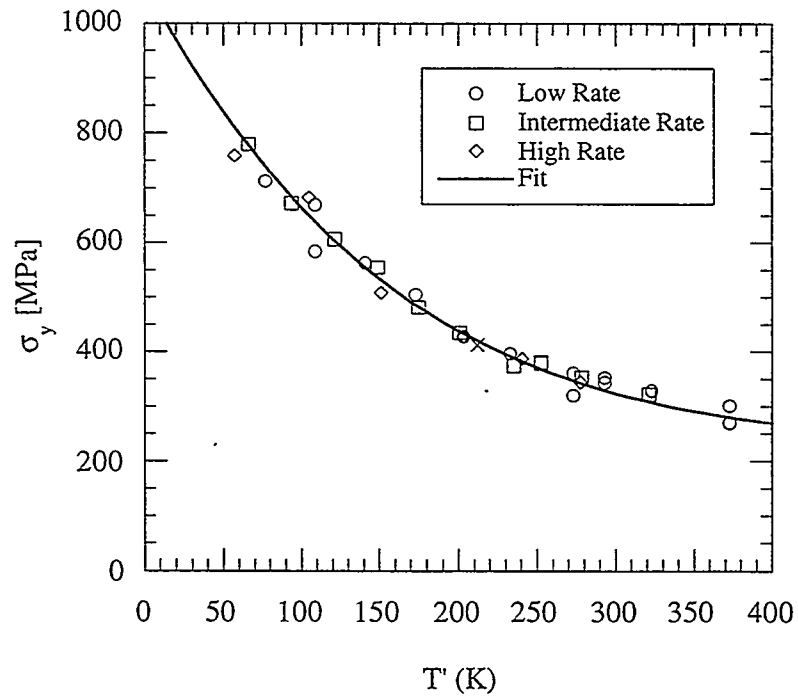


Figure 1. Plot of σ_y versus T' for various strain rates. The two-component fit activate flow model is shown as the solid curve as described in the text.

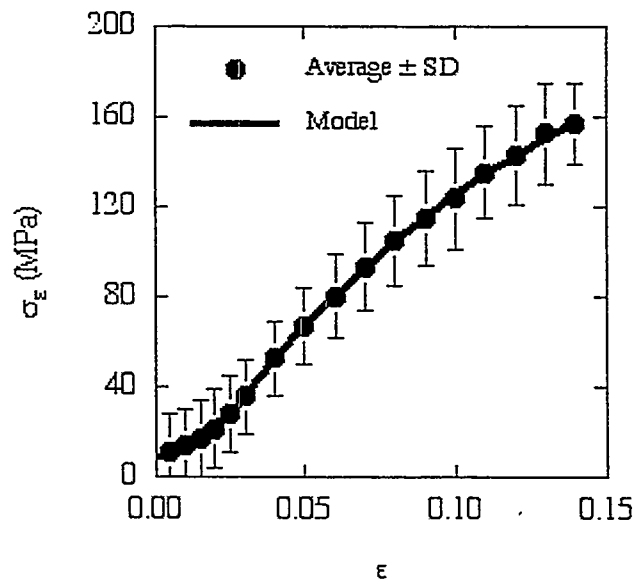


Figure 2. Plot of σ_ϵ , averaged for all T' , versus ϵ . The two-component Voce-type strain hardening model is shown as the solid curve as described in the text

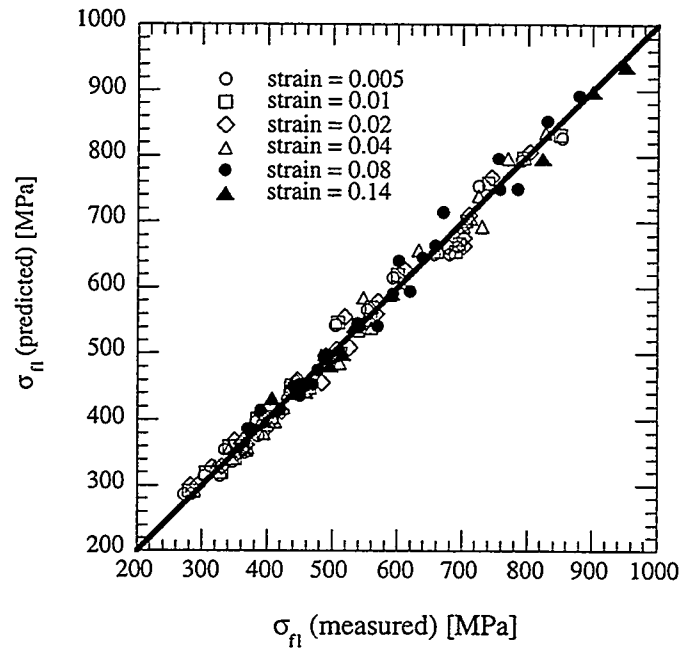


Figure 3. Comparison of the true flow stresses measured with those predicted by the model at true strains of 0.005, 0.01, 0.02, 0.04, 0.08, and 0.14.

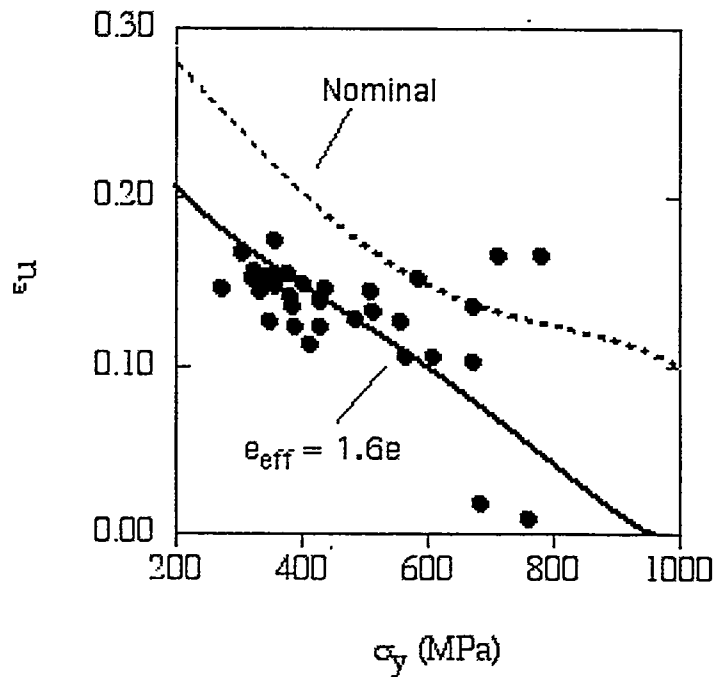


Figure 4. Plot of ϵ_u versus σ_y . Predictions of ϵ_u are shown as the solid and dashed curves as described in the text.

REFERENCES

1. E. Donahue, G.R. Odette, G.E. Lucas "A Generalized Constitutive Model For A V-4Cr-4Ti Alloy", *J. Nucl. Mat* (submitted ICFRM 9 proceedings)
2. H. M. Chung, H.-C. Tsai, D. L. Smith, R. Peterson, C. Curtis, C. Wojcik, R. Kinney, DOE/ER-0313/17, U. S. Department of Energy (1994).
3. M. L. Grossbeck, D. J. Alexander, J. J. Henry, W. S. Eatherly, L. T. Gibson, DOE/ER-0313/18, U. S. Department of Energy (1995).
4. A. N. Gubbi, A. F. Rowcliffe, W. W. Eatherly, DOE/ER-0313/18, U. S. Department of Energy (1995).
5. A. F. Rowcliffe, D. T. Hoelzer, S. J. Zinkle, DOE/ER-0313/26, U. S. Department of Energy (1999).
6. G. R. Odette, E. Donahue, G. E. Lucas, J. W. Sheckherd, DOE/ER-0313/20, U. S. Department of Energy (1996).
7. F. J. Zerilli, R. W. Armstrong, *J. Appl. Phys.*, 61 (1987) 1816.
8. M. Tang, B. Devincere, L. P. Kubin, *Modelling and Simulation in Materials Science and Engineering*, 7 (1999) 893.
9. J. P. Hirth, J. Lothe, *Theory of Dislocations*, McGraw-Hill, Inc., 1968.
10. P. Spatig, G. R. Odette G. E. Lucas, *J. Nucl. Mater.*, 217 (1999) 324.
11. E. Voce, *J. Inst. Metals*, 74 (1968) 537.